

Supporting Information for

Alkali-treated graphene oxide as a solid base catalyst: synthesis and electrochemical capacitance of graphene/carbon composite aerogels

Fanchang Meng, Xuetong Zhang,^{*} Bin Xu, Shufang Yue, Hui Guo and Yunjun Luo

School of Materials Science & Engineering, Beijing Institute of Technology, Beijing 100081, P. R. China

Research Institute of Chemical Defence, Beijing 100191, P. R. China

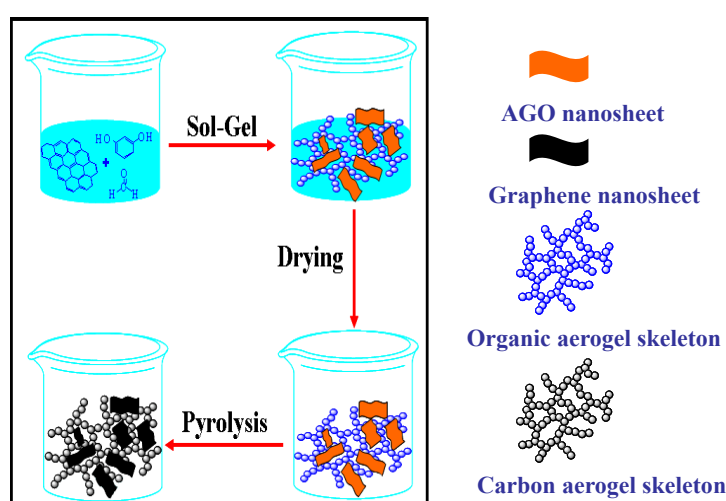
Aerospace Institute of Special Materials & Technology, China Aerospace Science & Industry Corp., Beijing 100074, P. R. China

Experimental

Materials: All reagents, including Resorcinol (99%) and formaldehyde (37% in water), absolute ethyl alcohol, sodium hydroxide (NaOH), TFA (trifluoroacetic acid) and acetone, were purchased from Beijing Chemical Reagents Company with their purity being of analytical grade and used as received. Graphene oxide (GO) was synthesized in our lab according to the procedure reported in our previous study (J. Mater. Chem., 2011, 21, 6494-6497).

Synthesis:

General procedure for synthesis of graphene/carbon composite aerogels is shown in Scheme 1. The details are as follows:



Scheme 1: The synthetic route for graphene/carbon composite aerogels

Synthesis of alkali treated graphene oxide (AGO): 23.7 mL NaOH aqueous solution (0.1 M) was added

into 17 mL of GO dispersion (7 mg/mL) with stirring for ca. 10 minutes, then AGO was coagulated and filtered from above mixture. Finally the solid AGO was washed repeatedly with ethanol, and then dialyzed with DI water at least over 3 times.

Synthesis of graphene/carbon composite aerogels: we have made products with different content of AGO in total solid content of 10 wt. %. All samples were with the molar ratio of resorcinol to formaldehyde of 0.5. Quantitative AGO with respective portion of 1.0, 2.0, 5.0, 10.0 wt. % of the total solid content was sonicated in an aqueous solution until homogeneous dispersion was obtained. If more GO, e. g., 15 wt. % of the total solid content, was added in, only inhomogeneous dispersion was obtained. Resorcinol (R) and Formaldehyde (F) were added in sequence into the AGO dispersion. The resulting mixture was then sealed and reacted in water bath at 80°C for 72 h. Then, the composite gel precursors were placed in solution of 0.125% TFA at 45°C for 3 days. The TFA wash assisted in further condensation of hydroxymethyl groups (-CH₂OH) remaining in the gels to form ether bridges between resorcinol molecules (Journal of Materials Science, 1989, 24, 3221-3227). The resulting gels were then removed from the TFA solution and soaked in acetone for 4 times (changing the acetone every 8 h) to exchange all the reaction media from the pores of the gel network. The wet gels were subsequently dried with supercritical CO₂ and pyrolyzed at 1000 °C (heating rate: 3 °C/min) under a N₂ atmosphere for 3 h, then the temperature was naturally lowered down to room temperature. Each final product keeping the original shape was recognized as a black cylindrical monolith.

Instrumentation: X-Ray photoelectron spectroscopy (XPS) was performed using an AXIS Ultra spectrometer with a high-performance Al monochromatic source operated at 15 kV. The XPS spectra were taken after all binding energies were referenced to the C 1s neutral carbon peak at 284.8 eV, and the elemental compositions were determined from peak area ratios after correction for the sensitivity factor for

each element. Rheological tests were conducted on a Physica MCR 301 Rheometer with 25mm diameter parallel-plate geometry. The gap distance between two plates was fixed to 2 mm and the frequency sweep was in the range from 0.1 to 100 rad/s at a fixed oscillatory strain of 0.2%. To avoid the solvent evaporation during the testing process, we used a plastic jacket to cover the hydrogel, and kept the test time as short as possible (~15 min) at the room temperature. Atomic force microscope (AFM, Veeco NanoScope III, Veeco Co., USA, operated in tapping mode) was used to characterize the surface topography of the samples. TEM was conducted at a FEI Tecnai 20 transmission electron microscopy. The imaging was performed at 200 kV. Nitrogen sorption measurements were performed with ASAP 2010 (Micromeritics, USA) to obtain pore properties such as the BET-specific surface area, pore size distribution, and total pore volume. Before measurement, the sample was outgassed under vacuum at 250°C for ca. 10 h until the pressure less than 0.665 Pa. UV-Vis spectroscopy was performed on UV-6100 double beam spectrophotometer (Shanghai Mapada). Fourier transformed infrared (FT-IR, Bruker Tensor 27) spectra were recorded between 400 and 4000 cm⁻¹. Raman spectra were recorded on a Renishaw system 1000 with a 50 mW He-Ne laser operating at 514.5 nm with a CCD detector. XRD patterns of samples were measured with a X'Pert Pro MPD (PANalytical, The Netherlands) diffractometer with monochromatic Cu K α 1 radiation ($\lambda = 1.5406 \text{ \AA}$) at 40 kV and 40 mA. The diffraction patterns were optimized with a step length of 0.01° (2θ) over an angular range 4.5-90° (2θ) with a scanning speed of 0.01°/s. The compression tests were carried out by a single-column system (FPZ100) with loading capacity from 100 to 1000 N at a constant loading speed of 1 mm/min. The electrochemical performances of the samples were measured in a two-electrode cell. The electrodes were prepared by pressing a mixture of 87 wt% of sample, 10 wt% of acetylene black and 3 wt% of PTFE binder into pellets (11 mm in diameter) and then drying at 120 °C for 12 h. The capacitor was assembled into two-electrode system, among which two electrodes were separated by polypropylene

membrane using 6 mol.L⁻¹ KOH aqueous solutions as electrolyte. The cyclic voltammetry (CV) was recorded by Solartron 1280B electrochemical workstation. The galvanostatic charge/discharge test was carried out on an Arbin cell tester (CT2001A) between 0 and 1 V. The specific capacitance (C) of a single electrode was determined with the formula $C = 2It/\DeltaVm$, where I is the discharge current (A), t is the discharge time (s), ΔV is the potential change in discharge (V) and m is the mass of the active material in a single electrode (g). A Keithley 4200 Semiconductor Characterization System was used to measure electrical conductivities (four-probe method) of the samples. Furthermore, the density of the resulting products calculated in Table 1 was determined as the mass of the aerogel divided by its volume, and the porosity of the resulting products was calculated as $(1 - \frac{\rho}{2.2}) \times 100$, where 2.2 (in the unit of g/cm³) means the density of the graphite.

Figures

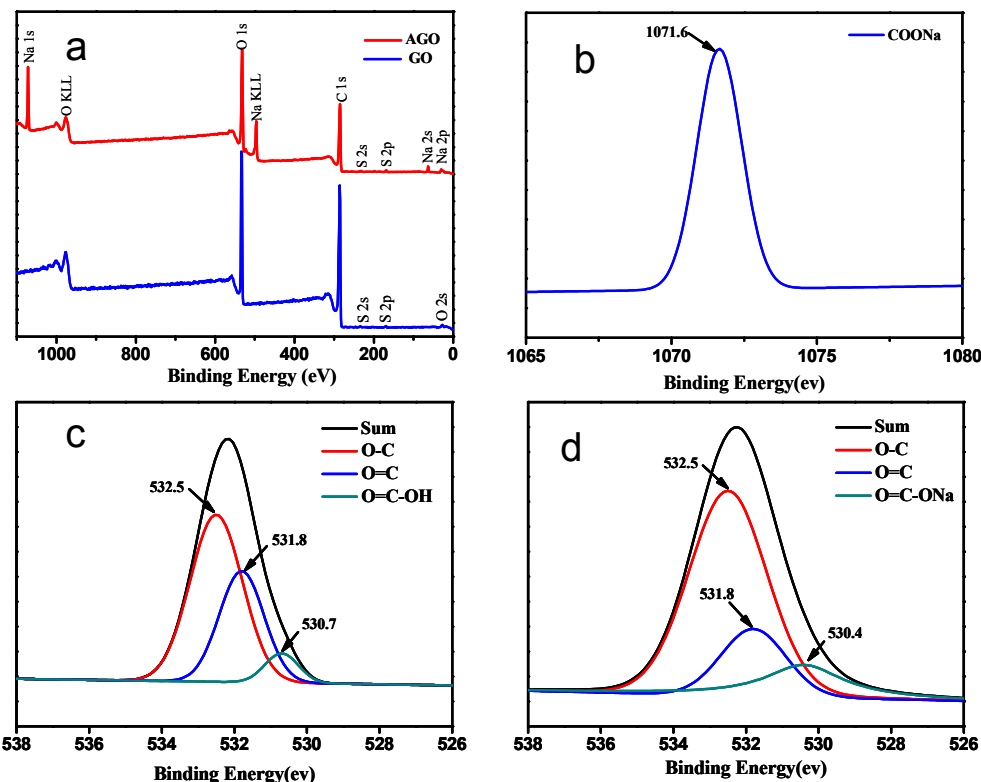


Fig. SI1 (a) full scan spectra of GO and AGO. Elements for GO: O: 32.44%, C: 65.97%, S: 1.48%, Cl: 0.11%. Elements for AGO: O: 26.32%, C: 67.71%, S: 0.47%, Cl: 0.19%, Na: 5.31%. (b) high-resolution Na 1s XPS spectrum of AGO, (c) high-resolution O 1s XPS spectrum of GO and (d) high-resolution O 1s XPS spectrum of AGO.

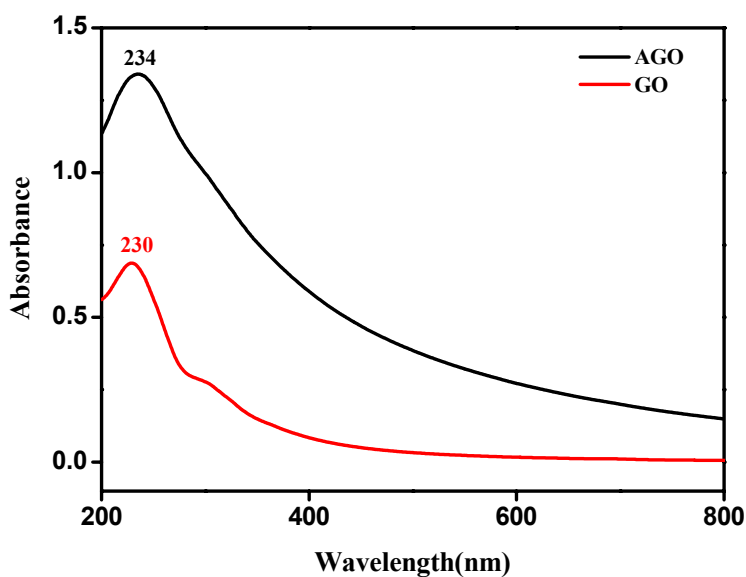


Fig. SI2 UV spectra of GO and AGO in ultra-pure water. The absorption peak of the GO at 230 nm slightly red-shifts to 234 nm, suggesting that the electronic conjugation within the graphene sheets is partially restored after treating with alkali as the partial reduction happened from graphene oxide to graphene in the presence of NaOH (please see ref. Adv. Mater. 2008, 20, 4490-4493).

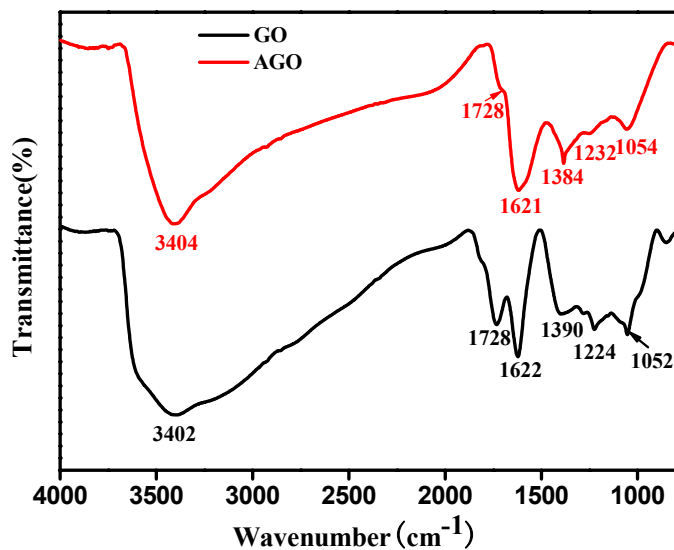


Fig. SI3 FT-IR spectra of GO and AGO. The peak at 3402 cm^{-1} shows a strong and broad absorption due to the $-\text{OH}$ stretching vibration (J. Phys. Chem, 2010, 114, 10368-10373), and an absorption band at 1728 cm^{-1} is typical of carbonyl stretching (Carbon, 2009, 47, 68-72). The peak at 1224 cm^{-1} due to C-OH stretching and one at 1052 cm^{-1} arises from C=O stretching, respectively (J. Phys. Chem. B, 2010, 114, 5723-5728).

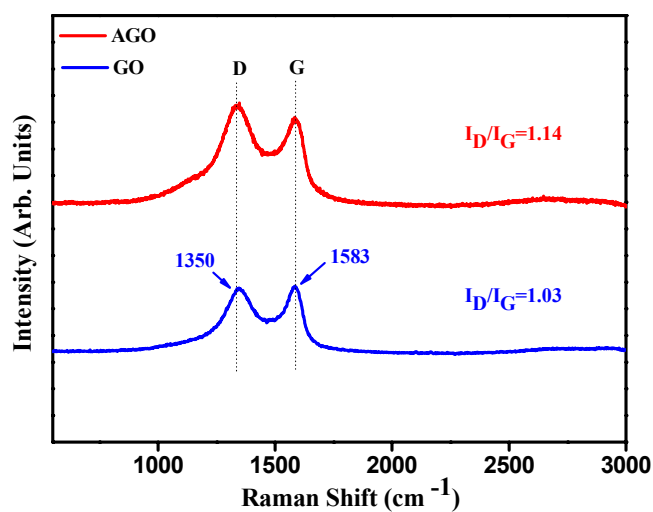


Fig. SI4 Raman spectra of GO and AGO. The relative intensity ratio I_D/I_G of AGO is higher than that of GO, resulting from a decrease in the average size of the sp^2 domains upon reduction of the exfoliated GO (Carbon, 2007, 45, 1558-1565).

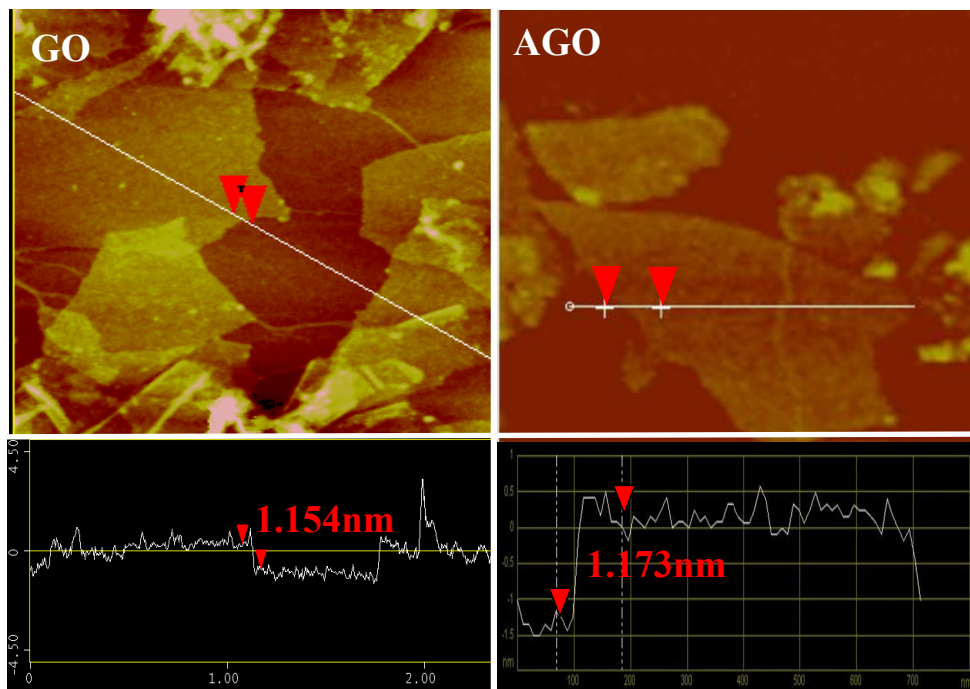


Fig. SI5 AFM images of GO (a, the same as Fig. SI1 (a) in ref. 6(a) of the manuscript) and AGO (b). The height (<1.2 nm) of both GO and AGO measured by AFM has confirmed the single-layer nature of the chemically modified graphene (Angew. Chem. Int. Ed. 2009, 48, 4785-4787).

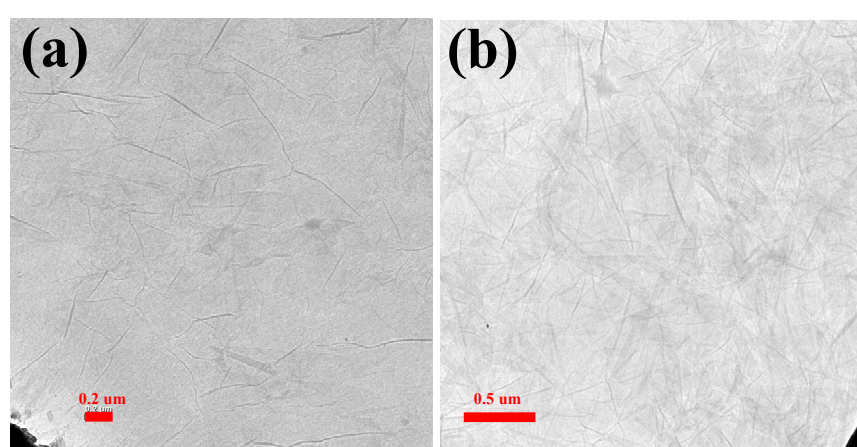
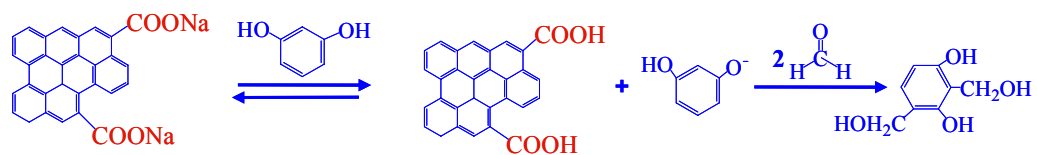


Fig. SI6 TEM images of GO (a, the same as the Fig. SI1(c) in ref. 6(a) of the manuscript) and AGO (b)

1. Addition Reaction



2. Condensation Reaction

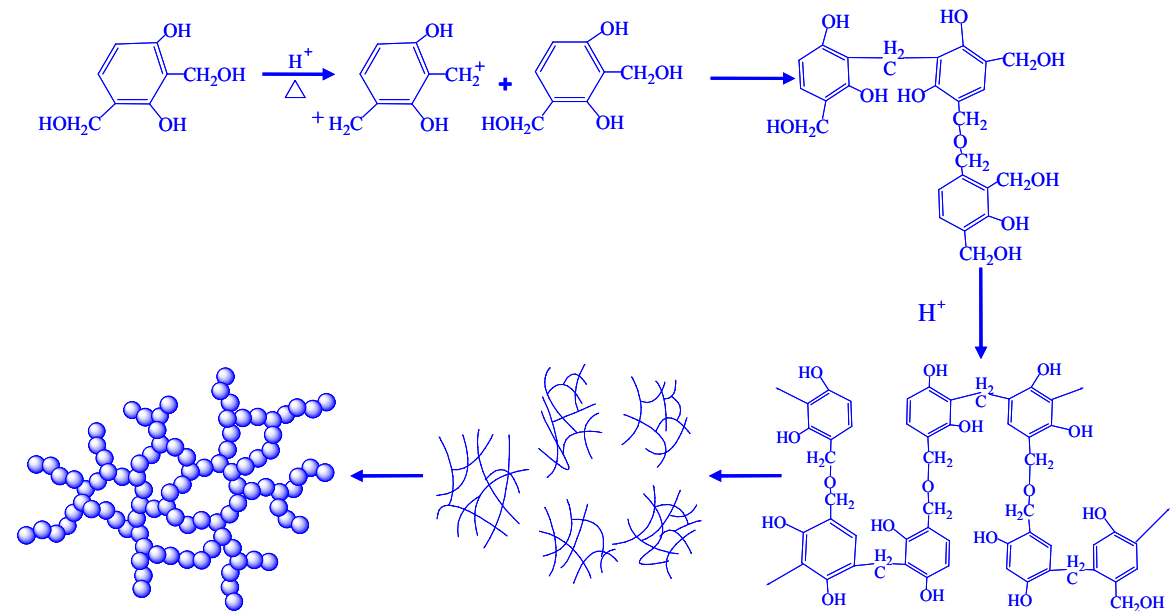


Fig. SI7 Proposed mechanism on polymerization of R with F in the presence of AGO as a solid base

catalyst, very similar to that of using NaCO_3 as a catalyst (see Adv. Mater., 2003, 15, 101-114).

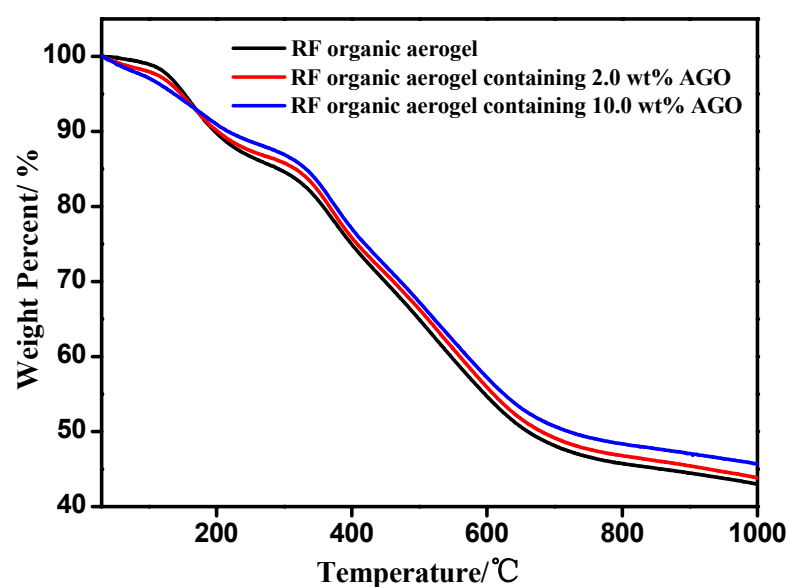


Fig. SI8 TGA curves of the RF aerogel and AGO/RF composite aerogels.

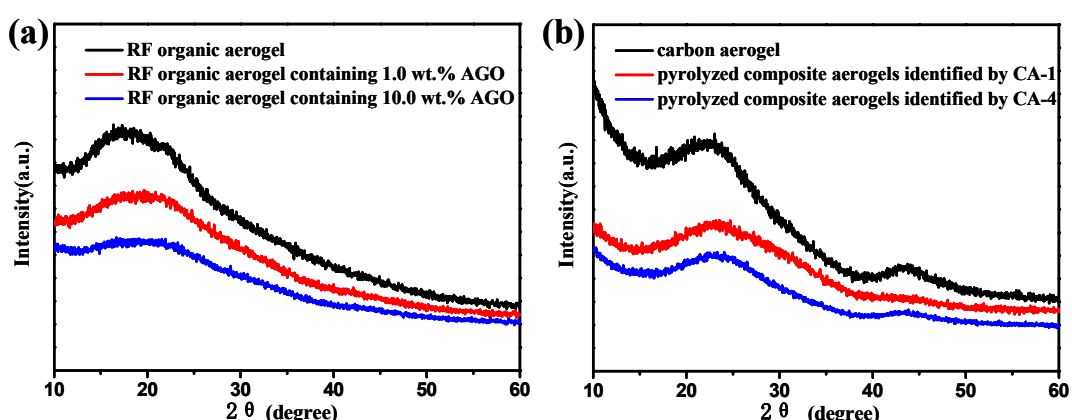


Fig. S19 XRD patterns of the composite aerogels before (a) and after (b) carbonization. No characteristic peaks of AGO in the composite aerogels before carbonization and peaks of graphene in the composite aerogels after carbonization indicate that AGO or graphene sheets were well dispersed in the organic or carbon matrix (similar deduction see ACS Nano, 2011, 5, 4720-4728).

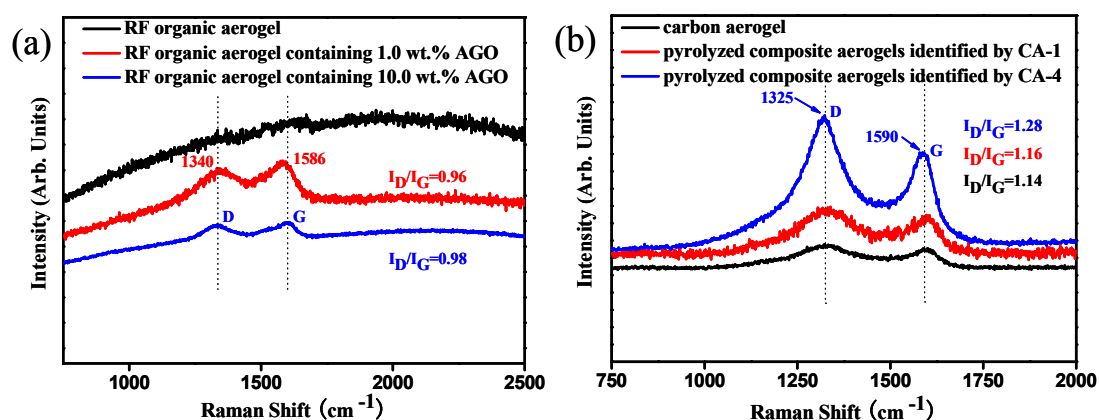


Fig. SI10 Raman spectra of the composite aerogels before carbonization (a) and after carbonization (b). The ratio of I_D/I_G was increased after carbonization, indicating that the AGO have been converted into graphene during carbonization (the intensity ratio of I_D/I_G for the pure graphene is 1.34 in our case).

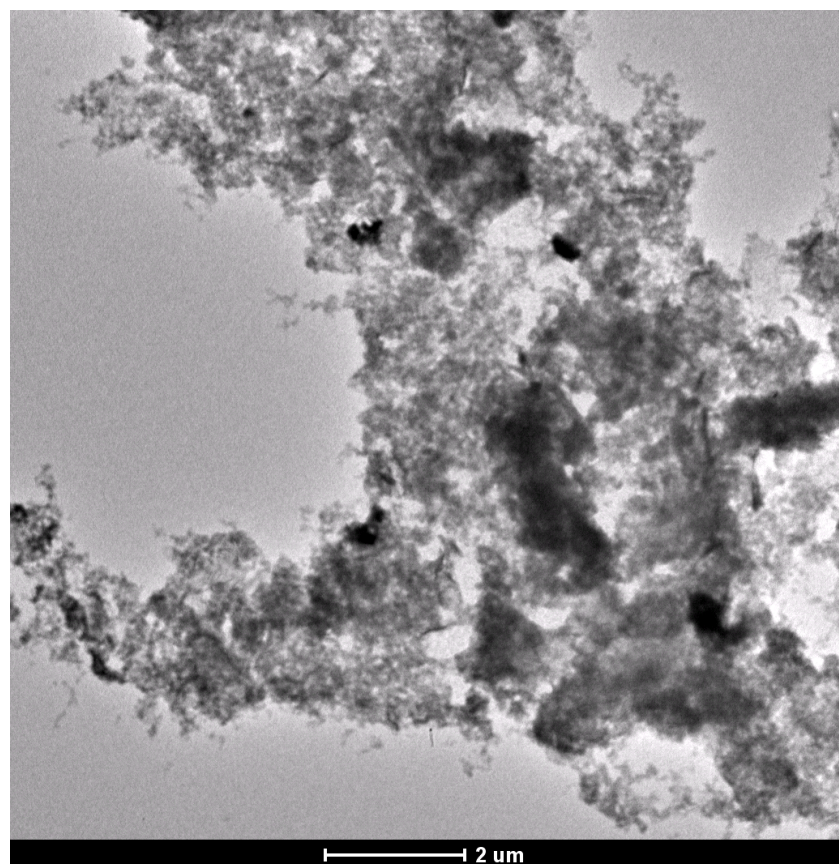


Fig. SI11 Low magnification TEM image of graphene/carbon composite aerogels

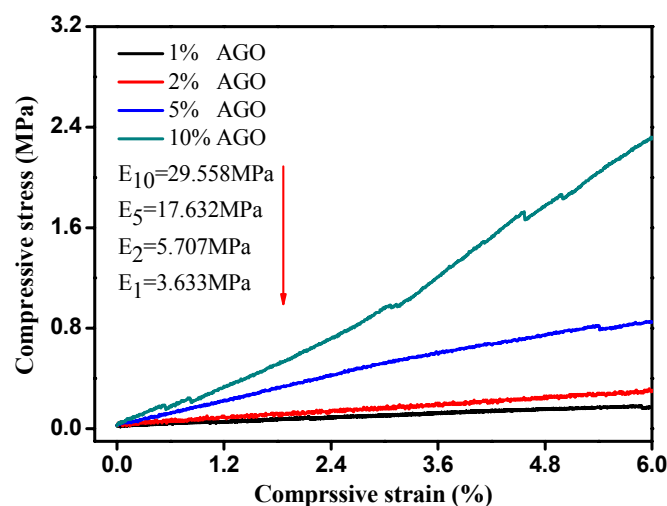


Fig. SI12 Compressive stress-strain curves of the resulting graphene/carbon composite aerogels with different amount of original AGO.